ISSN 1070-4272, Russian Journal of Applied Chemistry, 2017, Vol. 90, No. 8, pp. 1309−1314. © Pleiades Publishing, Ltd., 2017.

VARIOUS TECHNOLOGICAL PROCESSES

Photocatalytic and Photoelectrocatalytic Degradation of Metoprolol Tartrate in Aqueous Media by Recyclable Co Doping Fe_3O_4/TiO_2 Magnetic Core–Shell Nanocomposites[1]

M. Teimouri, S. Waqif-Husain, M. Saber-Tehrani*, and P. Abroomand-Azar

Department of Chemistry, Faculty of Science, Science and Research Branch, Islamic Azad University, Poonak-Hesarak, P.O.Box 14515-775, Tehran, Iran
**e-mail: drmsabertehrani@yahoo.com*

Received June 14, 2017

Abstract—Magnetically recoverable cobalt doping Fe_3O_4/TiO_2 magnetic nanocomposites with an acceptable core–shell structure were prepared via a sol-gel process at low calcination temperature. The crystalline size and structure, morphology, and magnetic properties of resulting particles have been characterized by X-ray diffraction (XRD), fourier transform infrared (FT-IR), FT-Raman, high-resolution transmission electron microscopy (HRTEM), scanning electron microscopy (SEM), energy dispersive X-ray spectroscopy (EDX), and vibrating sample magnetometry (VSM). Metoprolol tartrate (MET) as a pharmaceutical pollutant was used to observe the photocatalytic degradation ability of the magnetically recoverable particles. The process of degradation under UV irradiation at controlled temperature was studied and the remaining concentrations of MET as a contaminant were measured by UV-Vis spectrometer at $\lambda = 229$ nm. This ability remained 95.76% after three times of repetitive use at the same conditions. Various parameters such as reaction temperature, pH, and speed of stirring of the aqueous solution had an effect on the rate of degradation. The amount of cobalt dopant and nanocomposites are also effective on the rate of degradation. Coupling of electrical current with photocatalytic process has proven to be effective in the degradation of MET aqueous solution clearly.

DOI: 10.1134/S1070427217080195

INTRODUCTION

In the past two decades, pharmaceutical pollutions in environmental and water systems are recognized as hazardous problems [1–4]. It is necessary to remove pharmaceutical residues from wastewater by suitable methods to avoid their potential toxicity and other health impairments [5–8]. The photocatalytic oxidation of organic compounds using heterogeneous semiconductor nanophotocatalysis has been attracting great attention because of its high performance on the decontamination of aqueous media of various pollutants [9–11]. Nano-TiO_2 is an important catalysts with excellent photocatalytic activity [12–14]. Many researchers have reported that the photocatalytic efficiency of TiO_2 is dependent on crystalline phase, particle size, and specific surface area [15]. The sol-gel method is a useful process for preparing nano-TiO_2. This method offers advantages such as low-cost, low temperature synthesis, and control of the phase transformation (anatase, rutile and brookite) [16–19].

On the other hand, slight doping of TiO_2 with transition metals such as cobalt (Co^{2+}) has been widely investigated to show that the doped particle has a better photocatalytic ability [20–23]. One of the disadvantages of using these photocatalysts in sewage treatment plants is due to their weakness when recycling them because of their dispersive properties [9, 24, 25]. The use of Fe_3O_4 particles as a magnetic core in the Fe_3O_4/TiO_2 core–shell nanocomposites has been adopted to solve the problem [26, 27].

It is difficult to produce Fe_3O_4/TiO_2 core–shell nanophotocatalysts with acceptable UV light photoactivity and magnetic properties. This is because Fe_3O_4 particles can be oxidized at high calcination temperatures of Fe_3O_4/TiO_2 nanocomposites [28]. In present work, Fe_3O_4

[1] The text was submitted by the authors in English.

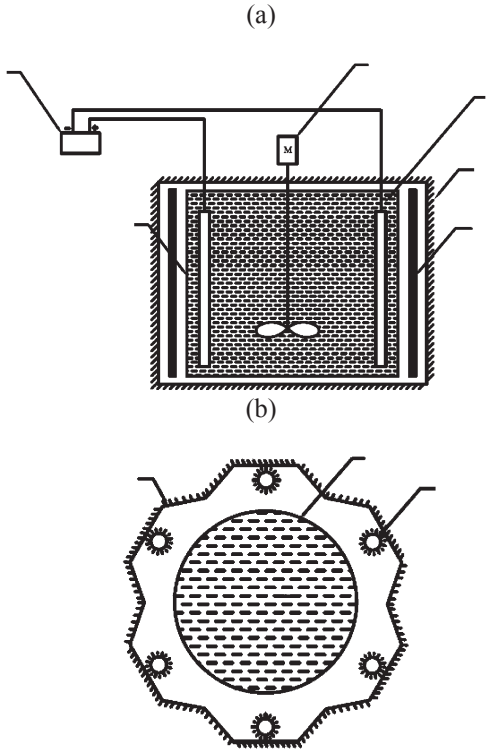

Fig. 1. Schematic diagram of photoelectronchemical reactor (a) front view (b) top view.

particles were prepared using a precipitation process in the first stage and recoverable Co^{2+} doping Fe_3O_4/TiO_2 core–shell nanophotocatalysts were synthesized via a modified sol-gel method in the second stage. Their photocatalytic efficiency under UV irradiation was studied for the degradation of Metoprolol tartrate (1-[4-(2-methoxyethyl) phenoxy]-3-(propan-2-ylamino) propan-2-ol tartrate (2 : 1), MET) which is a β-blocker that affects the heart and circulation. MET is used to treat angina and hypertension (high blood pressure). It is also used to treat or prevent heart attacks [3, 29]. The coupling of an electrochemical process with photocatalytic degradation has been suggested as a treatment option for removing pharmaceutical residues. The effects of a photoelectrocatalytic method on degradation of MET solution were studied.

EXPERIMENTAL

Synthesis and modification of Fe_3O_4 core particles. The magnetic Fe_3O_4 particles were prepared through a precipitation method. $FeCl_2 \cdot 4H_2O$ (1.49 g, Merck) and $FeCl_3 \cdot 6H_2O$ (4.05 g, Merck) were dissolved in 10 mL deionized water separately. The two solutions were mixed together and diluted to 1000 mL. Ammonia solution (25%, Merck) was added dropwise and the pH of reaction solution was maintained at 9–10. The final solution was stirred for 2 h. The black product was collected with a magnet and washed with deionized water several times.

Surface modification of Fe_3O_4 particles was carried out by reacting them with citric acid solution (500 mL, 0.2 M). The mixture of Fe_3O_4 particles and citric acid solution were kept under ultrasonic irradiation (Elma-S30H) for 30 min. The Fe_3O_4 precipitate was separated by magnetic field and was washed with deionized water/acetone several times. Finally, it was filtered and dried at 50°C.

Preparation of Co doping Fe_3O_4/TiO_2 composites. To synthesise the best Co doping Fe_3O_4/TiO_2 magnetic core–shell nanocomposites, 5 mL titanium(IV) isopropoxide (TTIP, 97%, Sigma-Aldrich) and 0.1 g hydroxy propyl cellulose (HPC, Wolfram) were dissolved in 100 mL ethanol solution (70%, Sigma-Aldrich) under stirring at 800 rpm (IKA-MAG @ RCT) and 50°C. HNO_3 was then added dropwise until the mixture solution fully dissolved and pH of the reaction solution was 4. Various amounts of $Co(NO_3)_2 \cdot 6H_2O$ (Merck) as a dopant (0.01, 0.015, 0.02, 0.03, 0.04, 0.05 wt %) were dissolved in 10 mL ethanol separately and were added to the first solution. Fine Fe_3O_4 particles (2.15 g) were mixed in sol and it was stirred for 40 min by a homogenizer (IKA-Ultra Turrax). The resultant mixture was dispersed using an ultrasonic bath for 30 min at 40°C. A gel was formed and dried at 60°C. Finally, it was calcined (Heraeus- D6450 Hanau) at 400°C for 3 h.

Photocatalytic activity measurements. The photocatalytic activity of Co doping Fe_3O_4/TiO_2 magnetic core–shell nanocomposites was studied by the chemical degradation of 50 ppm/500 mL Metoprolol tartrate salt (≥99%, Sigma-Aldrich) aqueous solution. The photocatalytic degradation of MET has been studied in the pH range of 2 to 11. According to results, the pH of the solution was adjusted to 9 and 0.1 g of the photocatalyst was added to it. Photocatalytic degradation was carried out in a photoelectrochemical reactor (electrical supply switched off). The scheme and details of reactor are shown in Fig. 1.

The reaction suspension was continuously stirred in the dark for 2 h. After turning on the UV lamps, 5 mL of the suspension was sampled every 10 min. The catalyst was then separated by magnetic field and centrifugation

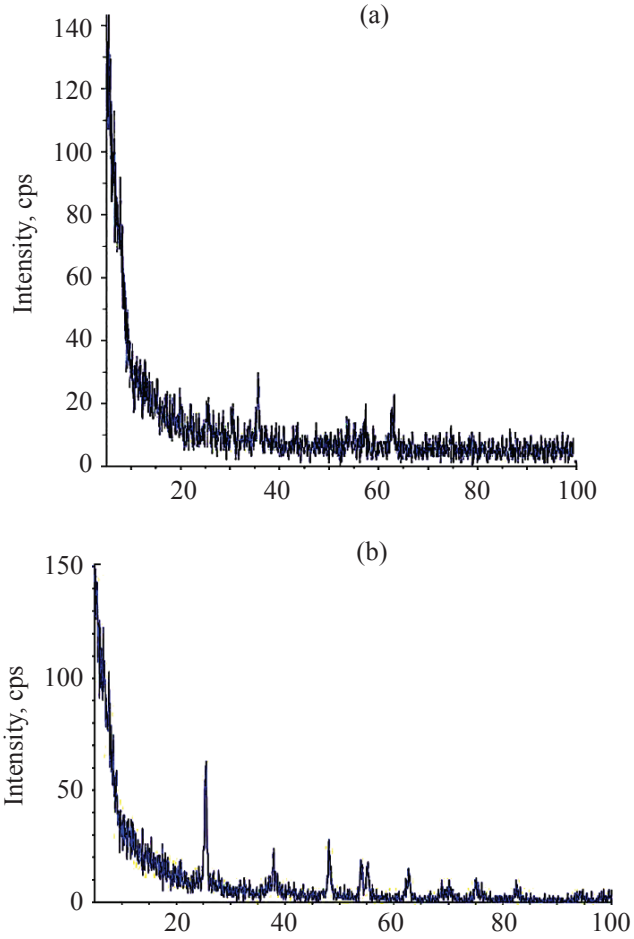

Fig. 2. XRD patterns of (a) 0.03 wt % Co doping Fe_3O_4/TiO_2 nanocomposites, and (b) pure TiO_2.

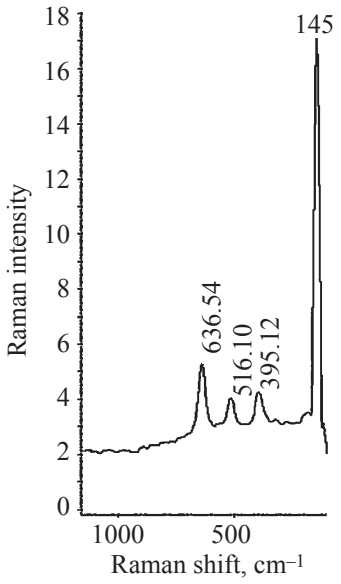

Fig. 3. FT-Raman spectrum of pure TiO_2.

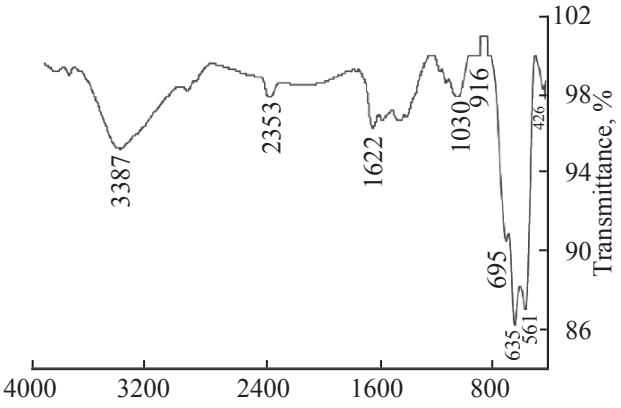

Fig. 4. FT-IR spectrum of 0.03 wt % Co doping Fe_3O_4/TiO_2 nanocomposites.

(Heraeus-Sepatech). Reduction of the MET concentration during UV light radiation was measured by Perkin Elmer lambda 2 UV/Vis spectrometer at λ_{max} = 229 nm after filtration through a millipore filter.

Photoelectrocatalytic degradation. For simultaneous electrochemical and photocatalytic (photoelectrocatalytic) degradation of MET by 0.03 wt % Co doping Fe_3O_4/TiO_2 nanocomposite (the optimal weight ratio of Co was 0.03 wt % with the lowest time for the degradation), the electrical system was joined to the photoreactor. Two stainless steel plates (of dimension 15 cm × 0.5 cm × 0.2 cm) were used as the electrodes. A direct current (DC) power source (12V) was connected to the cell. Samples were taken each 10 min and measured like before.

Characterization. The crystallographic patterns were performed by X-ray diffractometer (Seifert-3003 PTS), using CuK_α irradiation. Thermo Nicolet Nexus 870 FT-IR and Thermo Nicolet 960 FT-Raman were used for recording FT-IR and FT-Raman spectra of the samples. The core–shell structure of nanocomposites were carried out using a HRTEM (Philips CM30-300kv). The surface morphology, particle size, and distribution of the catalyst were observed by SEM (KYKY-EM3200) equipped with EDX spectrometer (Oxford instruments). The magnetic properties of particles were analyzed by VSM measurement (MDKFT) at room temperature.

RESULTS AND DISCUSSION

Characteristics of 0.03 wt % Co doping Fe_3O_4/TiO_2 magnetic core–shell nanocomposites. Figure 2 gives the XRD patterns of 0.03 wt % Co doping Fe_3O_4/TiO_2

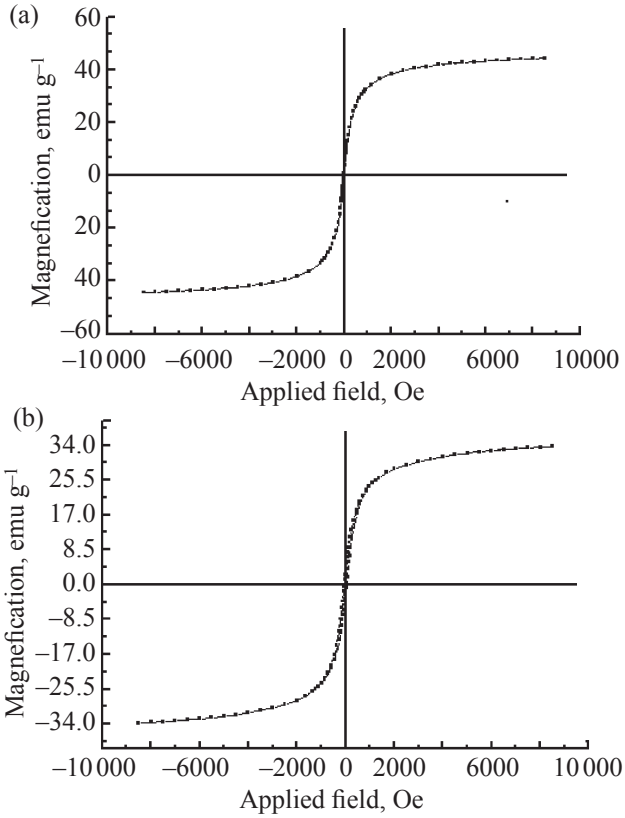

Fig. 5. Magnetic hysteresis curves of (a) Fe_3O_4 particles, and (b) 0.03wt% Co doping Fe_3O_4/TiO_2 nanocomposites.

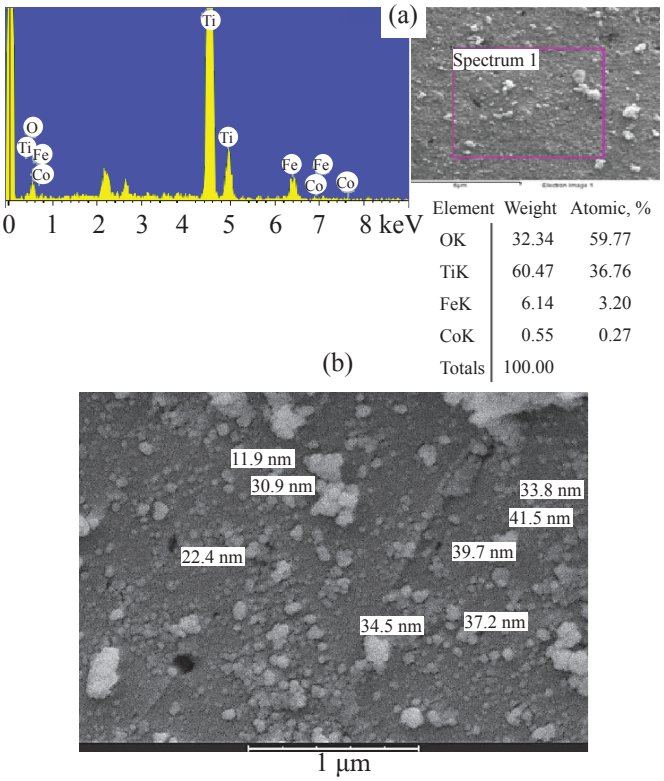

Fig. 6. (a) EDX spectrum 0.03 wt % Co doping Fe_3O_4/TiO_2 nanocomposites, (b) SEM image of 0.03 wt % Co doping Fe_3O_4/TiO_2 nanocomposites.

nanocomposites and pure TiO_2. According to the results, the crystal structure of 0.03 wt % Co doping Fe_3O_4/TiO_2 nanocomposites is similar to pure TiO_2 and the majority of the crystalline phase is anatase. The crystallite size of nanocomposites was calculated using the Debye–Scherrer equation, $D = k(\lambda/(\beta \cos \theta)$ (where k is a constant equal to 0.89, λ is the wavelength of X-ray, β is the full width at half the maximum height, and θ is the half diffraction angle) [10]. According to this equation, the average particle size was estimated to be about 25 nm.

FT-Raman spectrum of pure TiO_2 particles is shown in Fig. 3. The formation of the anatase structure was confirmed by FT-Raman spectroscopy, which showed almost all of the expected anatase vibrational modes at around 145, 395, 516, and 638 cm^{-1} [19, 30]. It is in agreement with XRD phase results.

Figure 4 shows FT-IR spectra of 0.03 wt % Co doping Fe_3O_4/TiO_2 core–shell nanocomposites in the range of 4000–400 cm^{-1}. The peaks in the region 400–700 cm^{-1} are attributed to the Ti–O and –O–Ti–O– flexion vibration [19]. The characteristic band for Fe–O stretching vibration is 561 cm^{-1} [31]. The bands at 916 and 1030 cm^{-1} are the characteristic vibrations of Ti–O–C group [32]. The peak at 2353 cm^{-1} is ascribed to the C–H bending vibration [26]. The absorption peaks in around 1622 and 3387 cm^{-1} are corresponded to the O–H vibrations of free water molecules and adsorbed water on nanocomposites surface [31, 33]. The peak between 500 and 600 cm^{-1} is assigned to cobalt dopant [34].

The magnetic hysteresis loops of 0.03 wt % Co doping Fe_3O_4/TiO_2 core–shell nanocomposites and Fe_3O_4 particles are shown in Fig. 5. As can be seen, the magnetic saturation (MS) of uncoated Fe_3O_4 (44.30 emu g^{-1}) is higher than core–shell nanocomposites (33.69 emu g^{-1}) but the coercive force of them is 0 Oe, so they have supermagnetic behavior. The magnetic property of Fe_3O_4 is very sensitive to the heating operation of the calcination process and the TiO_2 shell in the nanocomposite structure. It should be noted that magnetism is an important factor in the photocatalysis recycling process.

Morphological characterization of 0.03 wt % Co doping Fe_3O_4/TiO_2 core–shell nanocomposites was carried out by SEM, as shown in Fig. 6a. It can be seen that the nanocomposites have spherical morphology and

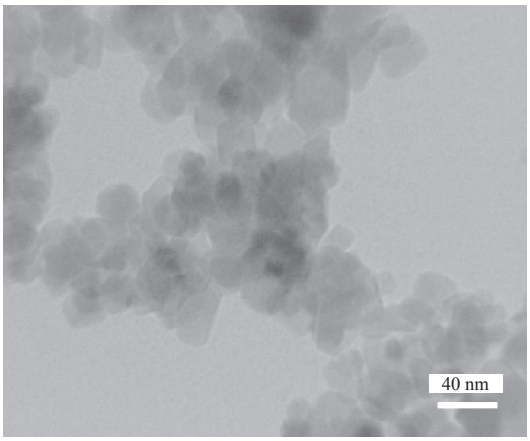

Fig. 7. TEM image of 0.03 wt % Co doping Fe_3O_4/TiO_2 nanocomposites.

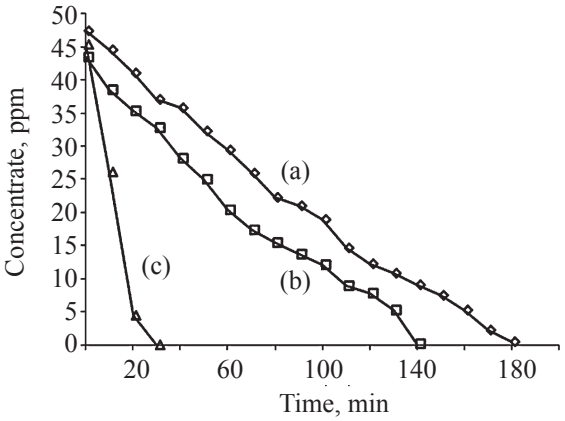

Fig. 8. Photodegradations of MET solution on (a) Fe_3O_4/TiO_2, (b) 0.03 wt % Co doping Fe_3O_4/TiO_2, and (c) photoelectrodegradation of MET solution over 0.03 wt % Co doping Fe_3O_4/TiO_2 nanocomposites (initial concentration 50 ppm; pH 9; *T* 40°C; catalyst dosage: 0.1 g).

in some places are relatively agglomerated.

By using EDX analysis, Ti, O, Fe and Co peaks are clearly seen in Fig. 6b, confirming the formation of 0.03 wt % Co doping Fe_3O_4/TiO_2 core–shell nanocomposites.

Figure 7 shows the TEM micrograph of 0.03 wt % Co doping Fe_3O_4/TiO_2 core–shell nanocomposites. A thin coating of TiO_2 (as a shell) onto the surface of the magnetic Fe_3O_4 particle (the core) resulted in the formation of a nanocomposite with core–shell type structure.

Photocatalysis efficiency of 0.03 wt % Co doping Fe_3O_4/TiO_2 magnetic core–shell nanocomposites. Figure 8 shows the relationship between irradiation time and the concentration of MET aqueous solution during photocatalysis and photoelectrocatalysis under UV light by 0.03 wt % Co doping Fe_3O_4/TiO_2 core–shell nanocomposites. It also compares the photodegradation of MET and Fe_3O_4/TiO_2 nanocomposites. The photocatalytic degradation of MET solution was carried out over 180 min in the presence of Fe_3O_4/TiO_2 nanocomposites. Furthermore, it can be seen from Fig. 8 that in the same optimum conditions, 50 ppm/500 mL MET solutions were degraded in 140 and 30 min for photocatalytic and photoelectrocatalytic processes using 0.03 wt % Co doping Fe_3O_4/TiO_2 core–shell nanocomposites respectively. It clearly shows that the direct electric current increases the rate of MET degradation sharply.

Used magnetic catalysts can be separated from the liquid media by a conventional external magnetic field and dried in an oven at 50°C. Its catalytic activity was studied in the same photocatalytic process three times. The photodegradation efficiency remained 95.76% after three cycles. Results are shown in Fig. 9.

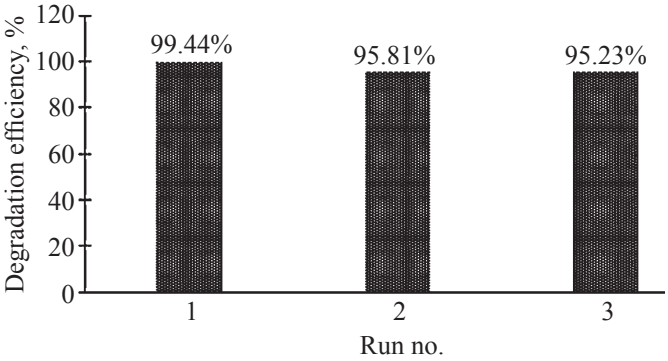

Fig. 9. Photodegradation efficiency (%) of MET solution on 0.03 wt % Co doping Fe_3O_4/TiO_2 nanocomposites after three times of repetitive use (initial concentration 50 ppm; pH 9; *T* 40°C; catalyst dosage: 0.1 g.

CONCLUSIONS

A modified sol–gel method for a facile synthesizing Co doping Fe_3O_4/TiO_2 nanocomposites with core–shell structure has been presented. The recovery problem of TiO_2 photocatalysis can be solved by magnetically separable Fe_3O_4 particles as the core of Fe_3O_4/TiO_2 nanocomposites. Also, cobalt as a dopant increases the photocatalytic performance of 0.03 wt % Co doping Fe_3O_4/TiO_2 nanocomposites. The nanoparticles have been characterized by XRD, FT-Raman, FT-IR, VSM, SEM, EDX, and TEM analysis. Coupling methods such as using electric current can provide a high photocatalytic activity

for photoelectrodegradation of MET in aqueous solution.

REFERENCES

1. Romero, V., Marco, P., Giménez, J., and Esplugas, S., *Int. J. Photoenergy*, 2013, vol. 2013, pp. 1–10.
2. Farzadkia, M., Bazrafshan, E., Esrafili, A., Yang, J.K., and Siboni, M.S., *Iran J. Environ. Health Sci. Eng.,* 2015, vol. 13, pp. 35–42.
3. Abramović, B., Kler, S., Šojić, D., Laušević, M., Radović, T., and Vione, D*., J. Hazard. Mater*., 2011, vol. 198, pp. 123–132.
4. Yang, H., An, T., Li, G., Song, W., Cooper, W.J., Luo, H., and Guo, X., *J. Hazard. Mater*., 2010, vol. 179, no. 1–3, pp. 834–839.
5. Sirés, I. and Brillas, E., *Environ. Int.*, 2012, vol. 40, pp. 212–229.
6. Arriaga, F.M., Esplugas, S., and Giménez, J., *Water Research*, 2008, vol. 42, no. 3, pp. 585–594.
7. Díaz, J.D.M., Joya, G., Utrilla, J.R., Ramos, R.L., Polo, M.S., García, M.A.F., and Castillo, N.A.M*., J. Colloid Interface Sci*., 2010, vol. 345, no. 2, pp. 481–490.
8. Choina, J., Kosslick, H., Fischer, C., Flechsig, G.U., Frunza, L., and Schulz, A., *Appl. Catal. B*, 2013, vol. 129, pp. 589 –598.
9. Li, C., Younesi, R., Cai, Y., Zhu, Y., Ma, M., and Zhu, J*., Appl. Catal. B*, 2014, vol. 156–157, pp. 314–322.
10. Hu, S., Li, F., Fan, Z., and Chang, C.C., *Appl. Surf. Sci*., 2011, vol. 258, no. 1, pp. 182–188.
11. Qourzal, S., Assabbane, A., and Ichou, Y.A., *J. Photochem. Photobiol. A*, 2004, vol. 163, no. 3, pp. 317–321.
12. Li, B., Wang, X., Yan, M., and Li, L., *Mater. Chem. Phys*., 2003, vol. 78, no. 1, pp. 184–188.
13. Akpan, U.G., and Hameed, B.H., *J. Hazard. Mater*., 2009, vol. 170, no. 2–3, pp. 520–529.
14. Zhang, D., *High Energ. Chem*., 2012, vol. 46, no. 3, pp. 206–211.
15. Bahadur, N., Jain, K., Srivastava, A.K., Gakhar, G.R., Haranath, D., and Dulat, M.S., *Mater. Chem. Phys*., 2010, vol. 124, no. 1, pp. 600–608.
16. Kontos, A.I., Likodimos, V., Stergiopoulos, T., Tsoukleris, D.S., and Falaras, P., *Chem. Mater*., 2009, vol. 21, no. 4, pp. 662–672.
17. Khanna, P.K., Singh, N., and Charan, S., *Mater. Lett.,* 2007, vol. 61, no. 25, pp. 4725–4730.
18. Wang, C., Böttcher, C., Bahnemann, D.W., and Dohrmann, J.K., *J. Mater. Chem*., 2003, vol. 13, no. 9, pp. 2322–2329.
19. Karthik, K., Pandian, S.K., and Jaya, N.V*., Appl. Surf. Sci*., 2010, vol. 256, no. 22, pp. 6829–6833.
20. Hamadanian, M., Vanani, A.R., and Majedi, A., *J. Iran Chem. Soc*., 2010, vol. 7, pp. S52– S58.
21. Minh, N.V., Hien, N.T.M., Vien, V., Kim, S.J., Noh, W.S., Yang, I., Dung, D.T., Khang, N.C., and Khoi, N.T*., J. Korean Phys. Soc*., 2008, vol. 52, no. 5, pp. 1629–1632.
22. Santara, B., Pal, B., and Giri, P.K., *J Appl. Phys*., doi: http://dx.doi.org/10.1063/1.3665883
23. Mugundan, S., Rajamannan, B., Viruthagiri, G., Shanmugam, N., Gobi, R., and Praveen, P., *Appl. Nanosci*., 2015, vol. 5, no. 4, pp. 449–456.
24. Zhu, H., Yang, B., Xu, J., Fu, Z., Wen, M., Guo, T., Fu, S., Zuo, J., and Zhang, S*., Appl. Catal. B*, 2009, vol. 90, no. 3–4, pp. 463–469.
25. Yang, L., Luo, S., Li, Y., Xiao, Y., Kang, Q., and Cai, Q., *Environ. Sci. Technol*., 2010, vol. 44, no. 19, pp. 7641–7646.
26. Xin, T., Ma, M., Zhang, H., Gu, J., Wang, S., Liu, M., and Zhang, Q., *Appl. Surf. Sci.,* 2014, vol. 288, pp. 51–59.
27. Pang, S.C., Kho, S.Y., and Chin, S.F., *J. Nanomater*., doi:10.1155/2012/427310
28. Kim, H.S., Kim, D., Kwak, B.S., Han, G.B., Um, M.H., and Kang, M., *Chem. Eng. J.,* 2014, vol. 243, pp. 272–279.
29. Šćepanović, M., Abramović, B., Golubović, A., Kler, S., Brojčin, M.G., Mitrović, Z.D., Babić, B., Matović, B., and Popovic, Z.V., *J. Sol-Gel Sci. Technol*., 2012, vol. 61, no. 2, pp. 390–402.
30. Rengaraj, S., Venkataraj, S., Yeon, J.W., Kim, Y., Li, X.Z., and Pang, G.K.H*., Appl. Catal. B.,* 2007, vol. 77, no. 1–2, pp. 157–165.
31. Niu, H., Wang, Q., Liang, H., Chen, M., Mao, C., Song, J., Zhang, S., Gao, Y., and Chen, C., *Materials*, 2014, vol. 7, no. 5, pp. 4034–4044.
32. Wei, J., Leng, C.J., Zhang, X., Li, W., Liu, Z.Y., and Shi, J., *J. Phys. Conf. Ser.,* doi 10.1088/1742-6596/149/1/012083
33. Behrad, F., Farimani, M.H.R., Shahtahmasebi, N., Roknabadi, M.R., and Karimipour, M., *EPJ Plus*, 2015, vol. 130, pp. 144–152.
34. Li, Y., Qiu, W., Qin, F., Fang, H., Hadjiev, V.G., Litvinov, D., and Bao, J., *J. Phys. Chem. C*., 2016, vol. 120, no. 8, pp. 4511–4516.